Japanese Journal of Applied Physics
Vol. 44, No. 7B, 2005, pp. 5791–5794

Fabrication of Silicon and Germanium Nanostructures by Combination of Hydrogen Plasma Dry Etching and VLS Mechanism

Ming-Che YANG, Jiann SHIEH*, Tsung-Shine KO[1], Hsuen-Li CHEN[2] and Tieh-Chi CHU[1]

National Nano Device Laboratories, Hsinchu 300, Taiwan, R.O.C.
[1]*Department of Atomic Science, National Tsing Hua University, Hsinchu 300, Taiwan, R.O.C.*
[2]*Department of Materials Science and Engineering, National Taiwan University, Taipei 100, Taiwan, R.O.C.*

(Received October 27, 2004; accepted April 21, 2005; published July 26, 2005)

Silicon and germanium nanostructures were fabricated by the combination of dry etching and vapor-liquid-solid (VLS) mechanism. Gold nanoparticles, about 20 nm in diameter, captured by self-assemble monolayer were adopted as the hard mask for dry etching and catalyst of germanium growth. Reactive ion etching in an inductive coupled plasma chemical vapor deposition (ICPCVD) system was used to fabricate various silicon nanostructures. Instead of CF_4, SF_6, and $SiCl_4$ gases, hydrogen plasma was used alone as the etching species to construct high-aspect-ratio silicon nanowires. Germanium nanostructures were then fabricated on the surface of silicon nanowires by dry etching and VLS mechanism.
[DOI: 10.1143/JJAP.44.5791]

KEYWORDS: ICPCVD, silicon nanowire, germanium nanostructure, hydrogen plasma etching, gold nanoparticle

1. Introduction

In comparison with zero- and two-dimensional nanostructures, the development of one-dimensional nanostructures has been slow until very recently. The difficulties in the fabrication and synthesis of these nanostructures include the good control of morphology and chemical composition. Since first discovered by Iijima,[1)] one-dimensional carbon nanotubes have become the focus intensive research because of its potential applications in mesoscopic physics and nanodevices. However, carbon nanotubes have two major shortcomings. First, the conductivity of carbon nanotubes is related to its chirality, but there is no effective method of controlling this structure. Second, the energy band gap is related to diameter that is easily influenced by fabrication parameters. Since semiconductor nanowires have fewer such problems, the methods of fabrication of semiconductor nanowires are receiving more attention.

Several processes have been developed for the fabrication of various kinds of nanowire, which are mainly divided into two main methods. One is the top-down lithographic method. The main problem of this method is the optical resolution limit, which can be overcome by high-energy direct-write electric-beam lithography at the expense of throughput. An alternative method is employing conventional lithographic techniques followed by oxidation and wet etching to reduce silicon diameter,[2)] but this method is not appropriate for other materials. Research has also been carried out to develop simpler methods; nanosized hard masks fabricated using rough metal films,[3)] colloidal metal particles,[4,5)] size-selected metal clusters[6,7)] and polymer spheres[8–13)] have been employed in reactive ion etching (RIE) for fabricating nanowires. Recently, Hsu *et al.* have also stated that one nanometer tip of Si, Poly Si, GaN, and GaP can be fabricated using a SiC hard mask *in-situ*.[14)]

The other method utilizes the bottom-up vapor-liquid-solid (VLS) growth mechanism.[15)] The major advantage of this method is its simplicity and accessibility. A representative VLS process begins with the dissolution of gas species into the nanosized liquid droplets of a crystal metal alloy. A liquid droplet can be regarded as a catalyst for limiting the lateral growth of individual wires. When continuously applying environmental gases, liquid droplets are supersaturated with target materials, and the single-crystalline nanowires will be nucleated and grows. Composite nanowires with core-shell and superlattice heterostructures have been developed by altering conditions during growth.[16–18)] Only a few studies, however, have been carried out using dry etching and nanoparticle-assisted growth. In this study, we demonstrate that germanium can be deposited on the separated silicon nanotips. ICPCVD was performed to fabricate well-aligned silicon nanowires and germanium nanostructures by the combination of hydrogen plasma dry etching and VLS mechanism. Gold particles serve as the nano-hard mask for hydrogen plasma etching and are also employed to grow germanium nanostructures. The effects of process parameters such as etching time, bias power, the density of gold on silicon wire and the formation mechanism are investigated here.

2. Materials and Methods

2.1 Fabrication of colloidal gold particles

Silicon substrates were cleaned sequentially in the baths of acetone and isopropyl alcohol with ultrasonic agitation. It was then dipped into a solution of 3-aminopropyltriethoxysilane (APTES), which acts as a coupling agent between gold and the substrate. Then the substrate was soaked in an aqueous Au colloid solution for 10 s to 1 min. The density of colloidal gold can be changed by the time the sample was submerged.

2.2 Fabrication of Si nanowire

After coating colloidal gold particles, the substrate was transferred to the ICP-CVD system. Before etching and the deposition process, chamber was cleaned with by CF_4 and O_2 plasma. The chamber was then evacuated to a base pressure of 5×10^{-5} Torr. For silicon nanowire etching, a gas flow of 200 sccm H_2 was introduced and the reactor pressure was adjusted to 10 mTorr. Generally, the substrate holder was heated to 400°C and the temperature of the system was maintained for 5 min in order to reach a stable condition. Both the RF inductive and 300 Hz bias powers

*E-mail address: jshieh@mail.ndl.org.tw

were applied at the same time to ignite plasma for etching silicon.

2.3 Fabrication of Ge nanostructure

After a 10 min hydrogen plasma etching, 1 sccm GeH_4 and 200 sccm hydrogen gas were introduced into the chamber under a reactor pressure of 10 mTorr. The reactive parameters are the same as those for the fabrication of Si nanowires for germanium nanostructures.

2.4 Analysis methods

The morphology and microstructure of the silicon and germanium nanostructures were examined by scanning electron microscopy (SEM, JEOL, JSM 6500), and the microstructure was characterized by glancing-incident-angle X-ray diffraction (GIAXRD, Philips, X'Pert Pro).

3. Results and Discussion

The top view micrograph of Au nanoparticles formed following the 1 min immersion in gold solution is shown in Fig. 1. The nanoparticles are dispersed uniformly with a density of $9 \times 10^9\,cm^{-2}$ and the mean diameter is about 20 nm. Figure 2(a) presents the cross-sectional SEM image of Si nanowires obtained after the 10 min dry etching. A nanoparticle can be found on the top of one nanowire and it has nearly the same diameter as that of nanowire, indicating that Au is a hard mask appropriate for hydrogen plasma etching. The diameter of the nanowires depends on the size of Au nanoparticles, and the height of Si nanowires can be controlled by etching time. For a long etching time, the dimensions of the nanowires as well as Au nanoparticles changed, as shown in Figs. 2(b) and 2(c). The top of nanowires became sharper and the Au nanoparticles almost vanished. The morphology of nanowires was changed into nanotips at more than 10 min of plasma etching since the size of the Au hard mask decreased with etching time. Compared with another etching gas, the aspect ratio of silicon nanotips can be apparently improved to as high as 30 at a tip radius of about 5 nm.

A simple mechanism can be described as follows: after the deposition of colloidal gold nanoparticles, the sample is etched with hydrogen plasma. First, the plasma reaches the silicon substrate and reacts with it. The area not covered with gold nanoparticles is removed. With time the silicon nanowire protected by the gold mask is formed. At more than 10 min of plasma etching, the colloidal gold particles

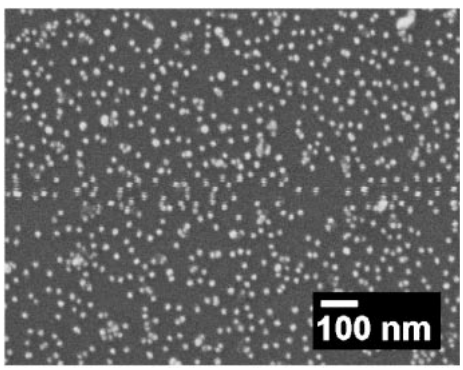

Fig. 1. SEM image of colloidal gold nanoparticles dispersed on silicon wafer following 1 min immersion in gold solution.

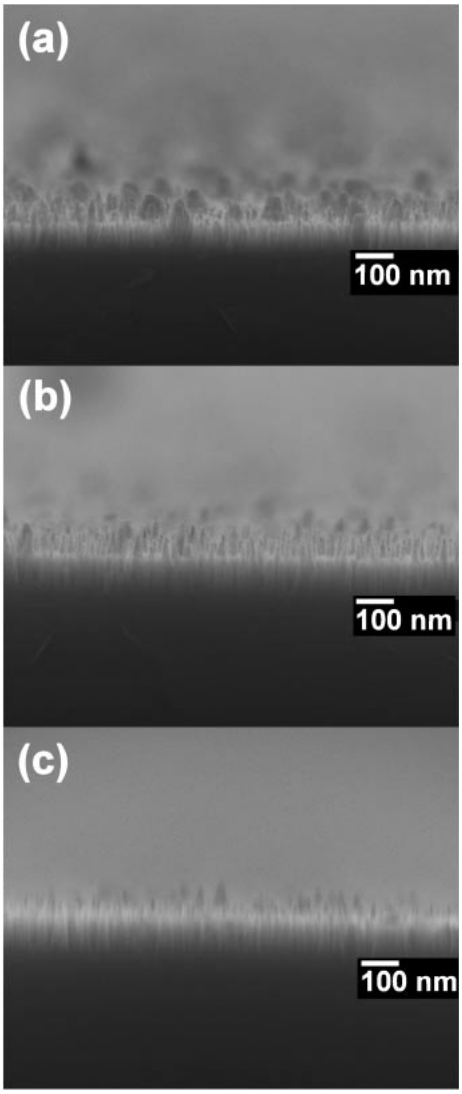

Fig. 2. SEM images of samples fabricated at 500 W inductive RF power and 300 W bias power at 400°C and different etching time (a) 10 min, (b) 20 min, (c) 30 min.

decrease in size as etching proceeds, which causes the exposed area of the substrate to increase. The conical silicon nanostructure is consequently constructed.

In general, CF_4, CHF_3, C_2F_6 or Cl_2 is employed as etching gas for silicon. Gases of low molecular weight such as CF_4 and CHF_3 have a high etching rate for silicon, but in the absence of the $(CF_2)_n$ polymer, the side wall is exposed to etching, which leads to the difficulty in forming high-aspect-ratio silicon nanowires due to the undercut effect. In order to obtain a fine isotropic etching, the addition of H_2, CO_2, and SF_6 gases is necessary. In addition to the complexity of this addition, these gases also immediately sputter gold particles as observed in our experiment. Accordingly, we propose that hydrogen gas is a good candidate having excellent selectivity of gold for silicon.

Hydrogen gas is seldom employed as etching gas, but recent research shows that hydrogen is a good etching gas for carbon nanotips or other carbon-based materials.[19] Moreover, there are studies showing that high-temperature hydrogen gas in the hot wire chemical vapor deposition (HWCVD) system can promote silicon etching.[20,21] With suitable fabrication parameters, hydrogen can be dissociated

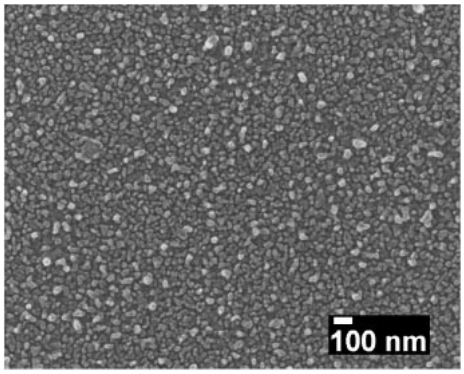

Fig. 3. Top-view SEM image of silicon substrate without bias.

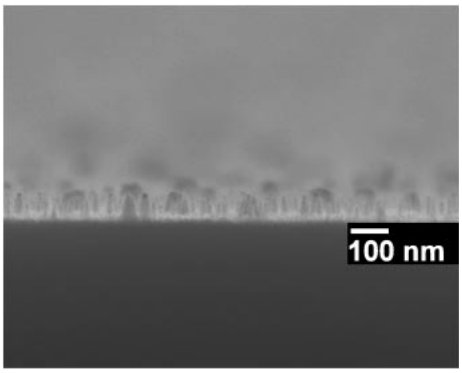

Fig. 4. SEM image of silicon nanowires after 10 s immersion in gold solution and 3 min dry etching.

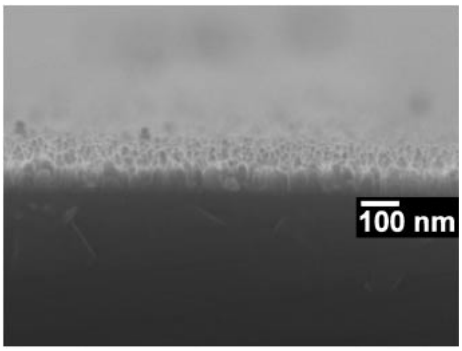

Fig. 5. SEM image of Ge-on-Si nanostructure.

and access the surface of the silicon substrate and transform Si–Si bonds into Si–H bonds. This bond strain relief results in a re-arrangement of sub-surface layers, which can induce the transformation of an etchable micro-crystalline Si layer. The rate of etching with hydrogen plasma also depends on the kind of silicon substrate. For example, a boron-doped silicon substrate promotes the formation of hydroboron radicals and decreases etching rate. We used a p-type silicon substrate and found that the etching rate for a silicon nanowire is 0.1 nm/s, which is close to that obtained by the HWCVD method. It can be shown that the ICP-CVD system used in this study also has the ability to dissociate hydrogen to etch silicon. Although the rate of etching Si nanostructures with hydrogen plasma is low, the excellent selectivity of this method can offset this drawback.

Without any bias, the etching reaction of silicon nanowires is not obvious. From a cross-section SEM image, we did not observe nanowires formed (not shown here), but very short silicon nanostructures can be found, as shown in Fig. 3. The likely mechanism for the behavior can be as follows. Hydrogen ion concentration increased with RF power; the ions can be attracted and accelerated by bias power. The acceleration of the ions increases the amount of active species on the substrate surface by collisions and thus enhance surface reactions.[22,23] Without applying bias, hydrogen ions may stay around the coil above the substrate and few positive ions are attracted to the substrate. Therefore, only short nanowires can be formed.

For the application in field emission, it is important to control the density of Si nanowires. By this method, the density of silicon nanowires can be changed by varying gold density. Figure 4 presents the cross-sectional SEM image of Si nanowires formed after 10 s immersion in gold solution and 3 min dry etching. The density of silicon nanowires is the same as that of colloidal gold nanoparticles, which shows that fabricating different-density silicon nanowires is easy by this method.

After hydrogen plasma etching for 10 min, Si nanowires were formed and gold nanoparticles were activated at the same time. The gold nanoparticles still exist on top of the silicon nanowire, as shown in Fig. 2(a). GeH_4 gas was then introduced into H_2 plasma to fabricate the Ge nanostructure. Figure 5 shows the SEM image of the Ge nanostructure. The nanowire length is apparently smaller than that in the case of without GeH_4 flow. This may arise from the observation that H_2 was consumed partially to react with GeH_4, thereby attenuating the etching effect. When adding GeH_4 and H_2 at the same time, three reactions may occur. One is that hydrogen plasma etches the silicon substrate, the other is that GeH_4 and H_2 gas at an appropriate ratio diffuse into gold droplets and the nucleation and growth of single-crystalline geranium nanowires occurs. Finally, the Ge film may be deposited on the silicon substrate directly.

To identify the Ge nanostructure, X-ray diffraction patterns were examined. Figure 6 shows the X-ray diffraction patterns of the Ge nanostructure obtained from different incident grazing angles. The intensity of the Ge (311) peak increased and that of the Si peak decreased as the grazing angle decreased from 3° to 1°, which indicates that the Ge nanostructure exists on top of the Si nanowire.

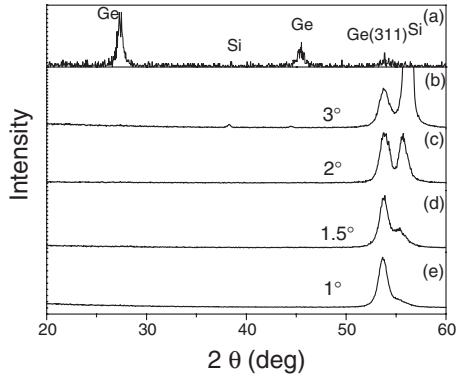

Fig. 6. X-ray diffraction patterns of Ge nanostructure at different incident grazing angles. (a) Ge film (b) 3° (c) 2° (d) 1.5° (e) 1°

Wang and Dai[24] stated that germane can undergo thermal decomposition, and Ge nanodots may not form as GeH_4 decomposition is suppressed by the increase in H_2 concentration. A low hydrogen ion concentration may provide few etching species for fabricating nanowires. However, as we decreased H_2 flow from 200 sccm to 100 sccm, the diameter and the height of nanowires at 100 sccm were not significantly different form those at 200 sccm, which indicates that H_2 concentration is not a critical parameter in the etching process.

Our previous studies showed that germanium nanoparticles can be successfully grown on the SiO_2 substrate using gold nanoparticles as the catalyst by the VLS mechanism. However, the nanoparticles tended to coalesce and form porous germanium.[25,26] Here, we can use separated silicon nanowires capped with gold nanoparticles to grow the germanium nanostructure without the coalescence phenomenon.

4. Conclusions

We have developed a simple and efficient method of fabricating aligned silicon nanowires and germanium nanostructures on a large-area substrate by hydrogen plasma dry etching and nanoparticle-assisted growth. Silicon nanowires and nanotips were manufactured by controlling the etching time of hydrogen plasma. The density of silicon nanowires can also be adjusted by the colloidal gold nanoparticles. Uniform, small-diameter, high-aspect-ratio and high-throughput nanowires can be realized simultaneously. Germanium-on-silicon nanotips were also synthesized successfully in this study. These nanostructures will be useful in many applications such as field emission displays and nanowire transistor devices.

Acknowledgments

The financial support from the National Science Council of Taiwan, Republic of China is acknowledged.

1) S. Iijima: Nature **356** (1991) 56.
2) P. B. Fischer and S. Y. Chou: Appl. Phys. Lett. **62** (1993) 1414.
3) K. Seeger and R. E. Palmer: Appl. Phys. Lett. **74** (1999) 1627.
4) P. A. Lewis, H. Ahemed and T. Sato: J. Vac. Sci. & Technol. B **16** (1998) 2938.
5) H. Park, S. Choi, S. Lee and K. H. Koh: J. Vac. Sci. & Technol. B **22** (2004) 1290.
6) T. Tada, T. Kanayama, K. Koga, P. Weibel, S. J. Carrol, K. Seeger and R. E. Palmer: J. Phys. D **31** (1998) L21.
7) V. Ovchinnikov, A. Malinin, S. Novikov and C. Tuovinen: Mater. Sci. Eng. B **69–70** (2000) 459.
8) J. C. Hulteen and R. P. Van Duyne: J. Vac. Sci. & Technol. A **13** (1995) 1553.
9) J. C. Hulteen, D. A. Terichel, M. T. Smith, M. L. Duval, T. R. Jensen and R. P. Van Duyne: J. Phys. Chem. B **103** (1999) 3854.
10) M. A. Wood, M. Riehle and C. D. W. Wilkinson: Microelectron. Eng. **57–58** (2001) 925.
11) M. A. Wood, M. Riehle and C. D. W. Wilkinson: Nanotechnology **13** (2002) 605.
12) K. Seeger and R. E. Palmer: J. Phys. D **32** (1999) L129.
13) M. Bale, A. J. Tuner and R. E. Palmer: J. Phys. D **35** (2002) L11.
14) C. H. Hsu, H. C. Lo, C. F. Chen, C. T. Wu, J. S. Hwang, D. Das, J. Tsai, L. C. Chen and K. H. Chen: Nano Lett. **4** (2004) 471.
15) Y. Xia, P. Yang and Y. Sun: Adv. Mater. **15** (2003) 353.
16) Y. Wu, R. Fan and P. Yang: Nano Lett. **2** (2002) 83.
17) M. T. Björk, B. J. Ohlsson, T. Sass, A. I. Persson, C. Thelander, M. H. Magnusson, K. Deppert, L. R. Wallenberg and L. Samuelson: Nano Lett. **2** (2002) 87.
18) L. J. Lauhon, M. S. Gudiksen, D. Wang and C. M. Lieber: Nature **420** (2002) 57.
19) W. J. Zhang, Y. Wu, C. Y. Chan, W. K. Wong, X. M. Meng, I. Bello, Y. Lifshitz and S. T. Lee: Diamond Relat. Mater. **13** (2004) 1037.
20) H. N. Wanka and M. B. Schubert: J. Phys. D **30** (1997) L28.
21) J. J. Boland and G. N. Parsons: Science **256** (1992) 1304.
22) J. H. Yen, I. C. Leu, C. C. Lin and M. H. Hon: Appl. Phys. A **80** (2005) 415.
23) C. L. Tsai, C. F. Chen and L. K. Wu: Appl. Phys. Lett. **81** (2002) 721.
24) D. Wang and H. Dai: Angew. Chem. Int. Ed. **114** (2002) 4977.
25) J. Shieh, T. S. Ko, H. L. Chen, B. T. Dai and T. C. Chu: Chem. Vap. Deposition **10** (2004) 265.
26) J. Shieh, H. L. Chen, T. S. Ko, H. C. Cheng and T. C. Chu: Adv. Mat. **16** (2004) 1121.